IEEE Access
Multidisciplinary | Rapid Review | Open Access Journal

Received November 19, 2018, accepted December 13, 2018, date of publication December 19, 2018,
date of current version January 11, 2019.

Digital Object Identifier 10.1109/ACCESS.2018.2888591

Research on Series Arc Fault Detection Based on Higher-Order Cumulants

GUANGHAI BAO[1], RUN JIANG[1], AND DEJUN LIU[2]
[1]College of Electrical Engineering, Fuzhou University, Fuzhou 350108, China
[2]Quanzhou Power Supply Bureau of State Grid, Quanzhou 362000, China

Corresponding author: Guanghai Bao (19428733@qq.com)

ABSTRACT At present, the detection methods on series arc faults are mainly based on the current of the main circuit, which probably results in misjudgment because of the singularity of the normal working current in a nonlinear load. What's worse, is the arc fault characteristic in the small power branch is easily ignored in the current of the main circuit, which leads to missed judgment. To solve these problems, a detection method based on coupling signal acquisition and higher-order cumulant identification is presented, through the electromagnetic coupling mechanism of high frequency current. By analyzing the coupling signal of the high-frequency current and using the higher-order cumulant algorithm during arcing process, the kurtosis of the coupling signal is calculated. In this paper, the unified threshold value on the kurtosis in various conditions is obtained. The results show that the novel method can be effectively used to detect and identify the series arc faults.

INDEX TERMS Coupling, higher-order cumulant, kurtosis, series arc faults.

I. INTRODUCTION

It is easy to cause an arc fault because of the complicated power system lines and the frequent switching action, which leads to loose electrical connections, insulation carbonization and air breakdown. Arc faults are the significant cause of fire hazards. According to the statistics of the 2015 China Fire Yearbook, the number of fires due to electrical causes accounted for 31.4% of the total number of fires [1]. Research by the U.S. Fire Administration (USFA) shows that approximately 46,500 fire accidents occurred in residences due to short circuits or arc faults in appliances [2]. Arc faults can be classified into three types: series arc faults, parallel arc faults and earth arc faults. Among them, due to the limit of the load in the line, the current of series arc faults is lower than the normal working current [3], which makes protection devices, such as a circuit breaker, difficult to provide effective protection. Therefore, it is of significance to study the characteristics of series arc faults and identify them correctly.

Presently, the main detection methods of series arc faults are described as follows:

By the physical characteristics of the arcing discharge, such as sound, light, heat, electromagnetic phenomena and radiation [4]–[6]; this method is susceptible to the limit of arc location, which results in low feasibility in practical applications. There are many patents on arcing detection and all of them, making use of the analysis of current or other indicators, extract signal from only one line (some examples of this method can be spotted in U.S. PAT. No. 6 972 572, U.S. PAT. No. 5 280 404, U.S. PAT. No. 5 185 684, U.S. PAT. No. 5 590 012, U.S. PAT. No. 9939481). Artale *et al.* [7] have proposed the chirp zeta transform (CZT) algorithm on analysis of low-frequency harmonic current which is different from fast Fourier transformation (FFT) because the former allows a better spectral resolution in a smaller frequency band, but CZT and a series of indicators to recognize the arc faults still cause unwanted trips and failures to trip. Recent research analyses arcing process by means of many novel algorithms and instruments, such as power spectral density in log spectral distance, Hilbert fractal antenna and so on [8], [9].Through detecting the main circuit current and analyzing it from both the time domain and the frequency domain, [10] analyzes the change of RMS value of line current during arcing process. [11] uses the change of the fifth harmonic amplitude of the line current to detect the presence of arcing. Reference [12]–[14] are based on the correlation coefficients and detect changes due to the presence of arc faults in the signal shape. In [15], algebraic derivatives of line currents are used as a feature for the arc fault detection. In [16], the wavelet packet technology is used to decompose, reconstruct and normalize the current signal. The spectral

characteristics of the arc faults are studied by combining information entropy and short time Fourier transformation. In [17], the third-order burg autoregressive model is used to model the normal and arc current signals at an all-pole, and the arcs on the Euclidean distance squares are calculated. In [18] and [19], the wavelet transform and neural network are used to extract the initial eigenvector of the arc faults to optimize the network structure and improve the detection speed. In [20], the phase space reconstruction of the line current waveform is carried out, and the support vector machine (SVM) model is established by combining the information dimension and the zero crossing time of the arc current phase space.

It can be seen from the aforementioned references that the detection method on the main circuit current, which detects the current signal of the single line, generally uses the singularity characteristics of an arc current signal, such as the ''zero crossing time'', the current burst after the zero crossing time or harmonic components. However, there is a similar and singular characteristic in the rated current of the nonlinear load, which is easily confused with the arc characteristic. The arc characteristic in the small power branch is usually weak and easily ignored in the main circuit current, which results in failure-to-trip situations. Meanwhile, starting process of many loads tends to lead to unwanted trips for steep pulses. Therefore, this paper has proposed a novel method that is different from the aforementioned literature, putting the neutral line and the phase line together through the current transformer to collect the data of the coupling signal. By analyzing the electromagnetic coupling signal of the high-frequency current, the method uses the statistical tool on higher-order cumulants to calculate the kurtosis value of the coupling signal which can distinguish between the normal and the arcing clearly. The experimental results show that this novel method can effectively detect and identify the series arc faults.

II. ELECTROMAGNETIC COUPLING MECHANISM OF A HIGH-FREQUENCY CURRENT

AC arc current naturally goes down to zero every half cycle around a short period of time, and the current is limited to a small amplitude approximately equal to zero since the resistance in the arc gap becomes very large, which is often referred as the zero crossing time of the current [21]. It is the critical moment of the arc extinguishing and reigniting during the zero crossing time. Before the arc reaches the zero point, if the characteristic of the dielectric recovery strength is higher than that of the arc voltage recovery strength, the arc is extinguished and the current is reduced to zero. After the zero crossing, the voltage on the arc gap rises to the supply voltage, and the alternating voltage increases so that the arc is reignited and the arc current increases rapidly with the instantaneous reduction of high-impedance state of the arc.

The line current shows a great deal of instability when the arcing transient current emerges, and many high-frequency components will be superimposed on the time domain.

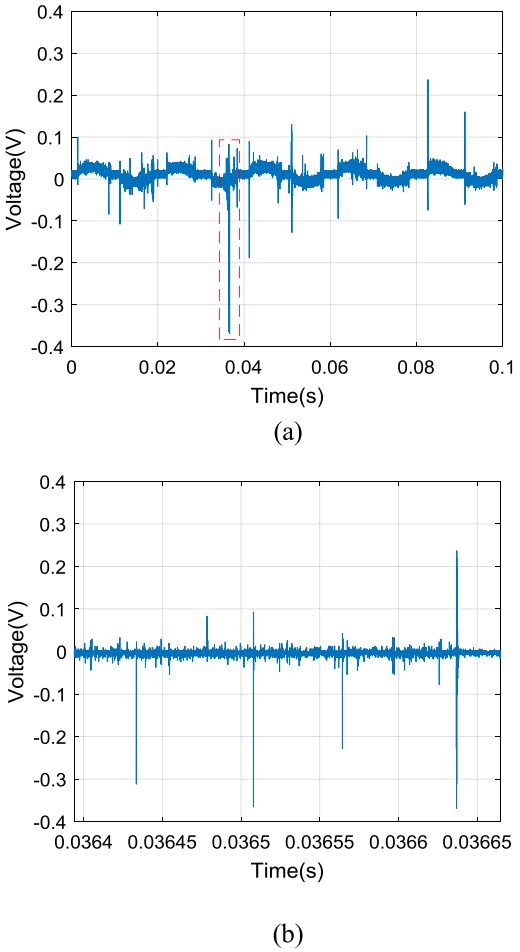

FIGURE 1. Analysis of arc high frequency current (transformed into the voltage output in the secondary circuit). (a) high-frequency current before and after the zero crossing time. (b) amplified analysis of the partial high-frequency current.

In other words, the high frequency current signal will appear in the line when the arc is extinguished and reignited, which is shown in Fig. 1, where Fig (b) shows the waveform of the amplified partial high-frequency signal.

According to the law of electromagnetic induction, the alternating current produces a changing magnetic field. If the currents on the two lines are equal in amplitude and opposite in direction, the magnetic field generated around the lines is shown in Fig. 2 (for easy analysis, the magnetic field generated by the black current is marked with black, while that generated by the red current is marked with red), where the current flowing to the right on the L line produces a vertical magnetic field out of the page above the L line and a vertical magnetic field into the page below the L line. The current flowing to the left on the N line is analyzed similarly. It can be found that the magnetic field on the outer side of the two lines is weakened by the two opposite magnetic induction lines, and the magnetic field in the middle of the lines is enhanced by the combined effect.

If the L line and the N line are put together through the transformer, the current signal is offset mutually, and the

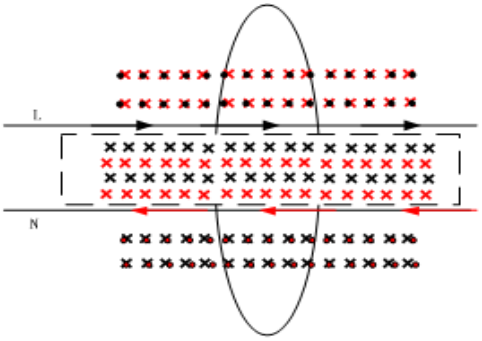

FIGURE 2. Magnetic field analysis of two power lines.

resulting magnetic field is very weak because of the low frequency of the normal current. The coupling effect of the transformer can be approximated as zero. However, when an arc fault occurs, the current contains many high frequency components, and the electromagnetic field generated by the arc current can be expressed as follows [22]:

$$E_{arc} = \frac{1}{4\pi\varepsilon_0 c^2}\frac{dI_{arc}}{dt} \tag{1}$$

where ε_0 is the dielectric constant of air and c stands for the speed of light.

As the high frequency current of the arc can reach the kHz or even the MHz level [3], [23], according to equation (1), a strong electromagnetic field will be generated around the wire, especially between the two wires. The high frequency electromagnetic field will be coupled to the coil in the transformer. In practice, the copper wire in the transformer cannot be completely wound around the coil. Additionally, the two power lines can not be completely parallel, and the magnetic field between the two wires will not be symmetrical along the centerline distribution, so the coupling signal will be enhanced.

Based on the above analysis, this paper collects the coupling signal through the transformer to identify the arc faults.

III. ANALYSIS OF THE ACQUISITION OBJECT

A. EXPERIMENT PLATFORM

The platform of the series arc faults is shown in Fig. 3, which includes two current transformers, an arc generator, a load, an AC source and an oscilloscope. The current transformer with a maximum bandwidth of 100MHz and a variable ratio of 1:400 is selected for the coupling signal acquisition of the two lines, with the characteristics of high sensitivity, being stable and a reliable output. A 1000 Ω resistor is in parallel with the output so that the current signal of the primary circuit is converted into the voltage output of the secondary circuit. According to the UL1699 standard, the arc generator can simulate the ac arc faults caused by loose connection when the two rods separate. The moving electrode is a copper rod with a diameter of 8 mm, and the fixed electrode is a carbon rod with a diameter of 8 mm. The experimental loads are divided into resistive loads (a 1800 W kettle and a 200W

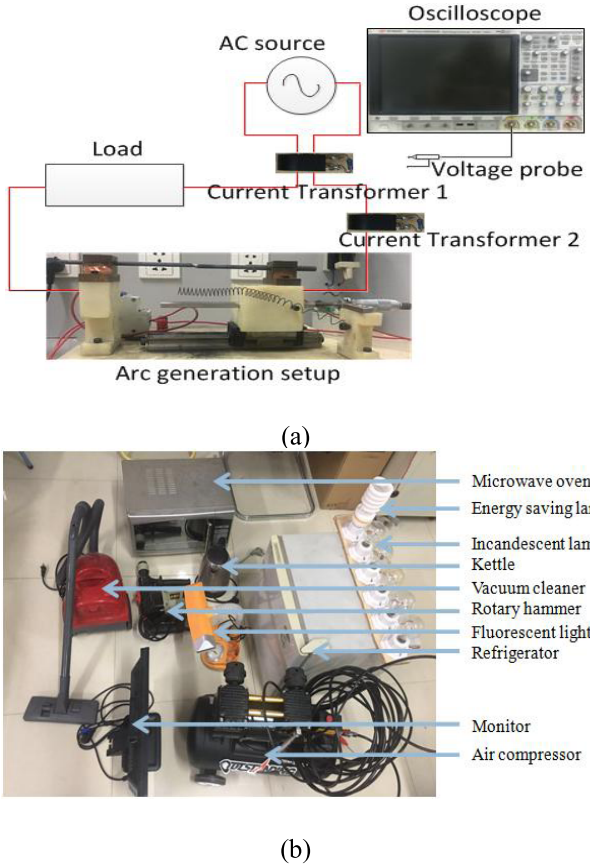

FIGURE 3. The experimental platform of series arc faults. (a) the main circuit. (b) experimental loads.

incandescent lamp), inductive loads (a 250W refrigerator and a 1200W rotary hammer) and non-linear loads (a 1500W microwave oven, a 1200W vacuum cleaner, a 200W monitor, a 85W energy saving lamp and a 11W fluorescent light). The oscilloscope with a bandwidth of 200MHz and a maximum sampling rate of 5GHz is used to acquire voltage data, and the voltage probe with a maximum amplitude of 300V and a bandwidth of 700MHz is used to measure rapid changing pulse of arc voltage.

B. ANALYSIS OF COUPLING SIGNAL ACQUISITION ADVANTAGES

To overcome the shortcomings of the present detection method, the situations of missed and faulty judgment are analyzed by comparing the main circuit current with the coupling signal, and the experimental platform is shown in Fig. 3.

1) ANALYSIS OF THE MISJUDGMENT SITUATION

The arc-like waveforms of the main circuit current and the coupling signal analysis are shown in Fig. 4. Fig (a) shows that the normal current of the microwave oven is very similar to the arcing current of the same load. There are some general characteristics under the main circuit current when arc faults generate, such as the ''zero crossing phenomenon'', the rising

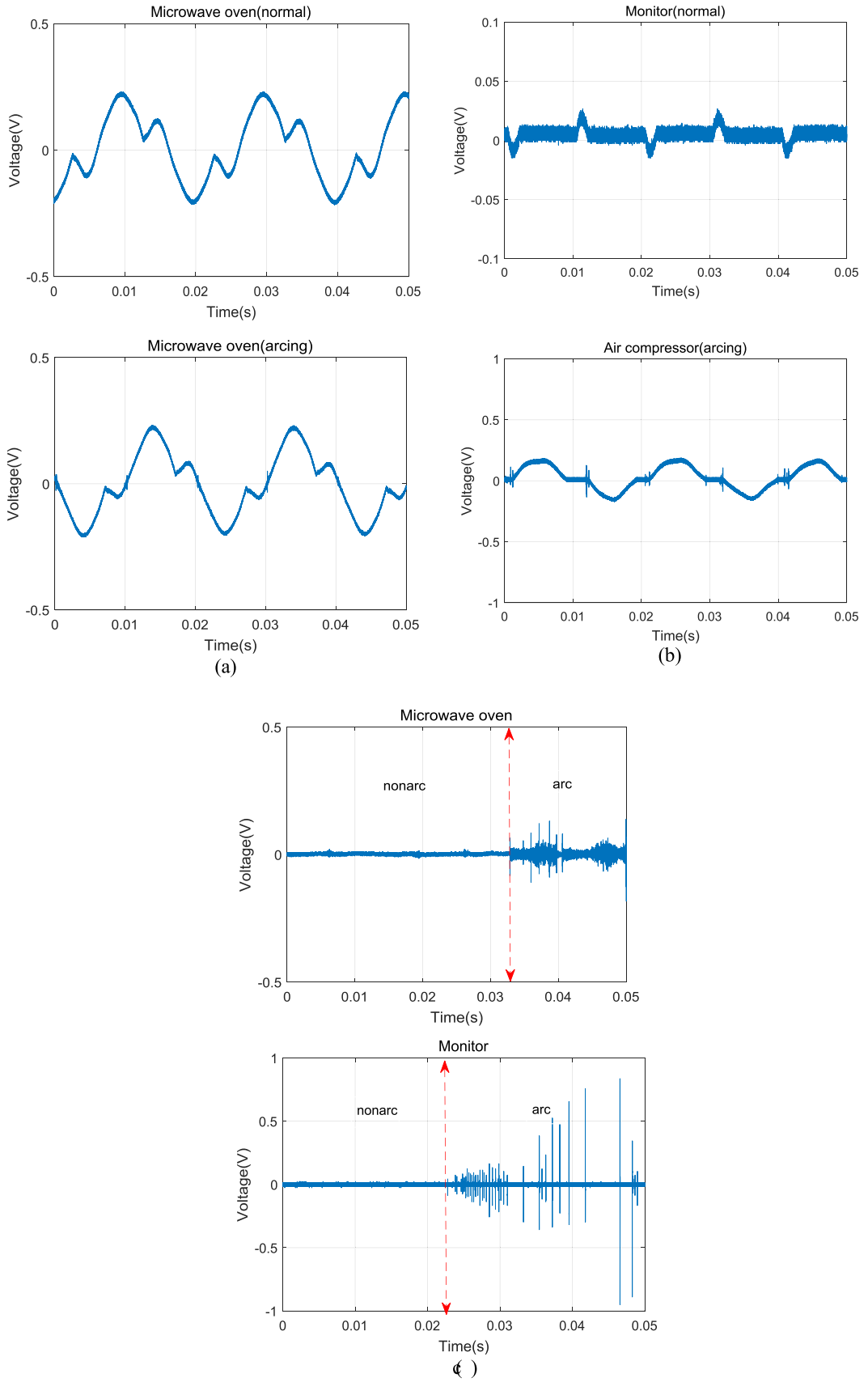

FIGURE 4. The waveform of the main circuit current and the coupling signal (transformed into the voltage output in the secondary circuit). (a) main circuit current. (b) main circuit current. (c) coupling signal.

rate after the zero crossing time, and the peak fluctuation. However, the rated current of some non-linear loads always appears to have similar characteristics to that of the arc. For example, there is the similar zero crossing phenomenon in the rated current waveform of the monitor, which is often confused with the arcing current waveform of the air compressor in Fig (b). Therefore, misjudgment is easy to appear if only the above arc characteristics are used. To improve the reliability of identification, it is unavoidable to carry out additional and more complex processing of non-linear loads under the present current detection method.

According to the analysis of Fig (c), the coupling signal acquisition method proposed in this paper has obvious advantages. Because the transformer current signal is offset mutually and the magnetic field generated by the low frequency alternating current is weak, which makes the coupling signal be approximately zero. This method is not subject to the singular current signal of various types of loads in a normal situation. When the arc faults occur in the circuit, the electromagnetic signal generated by the arc high frequency current is coupled to the measuring circuit through the transformer coil, showing a series of pulse waves, which is obviously contrasted with the normal signal waveform and helpful in the identification of the arc faults.

2) ANALYSIS OF THE MISSED JUDGMENT SITUATION

Fig. 5 shows the analysis of the signal waveform of the combined loads(a 1800W kettle and a 1200W rotary hammer). It can be seen from Fig (b) that the current waveform in the main circuit did not change significantly when the arc occurred in the relatively small power branch (a 1200W rotary hammer). The reason is that the arc signal is too weak to be ignored in the large current of the main circuit, which is likely to cause a missed judgment. In this paper, the characteristics of the arc faults from the coupling signal are more obvious than those of nonarc. This is because the high-frequency current of the low-power branch is converged to the main circuit, and the main circuit current also presents high-frequency characteristics so that the coupling signal produced by the high-frequency magnetic field can be detected and the problem of missed judgment can be solved.

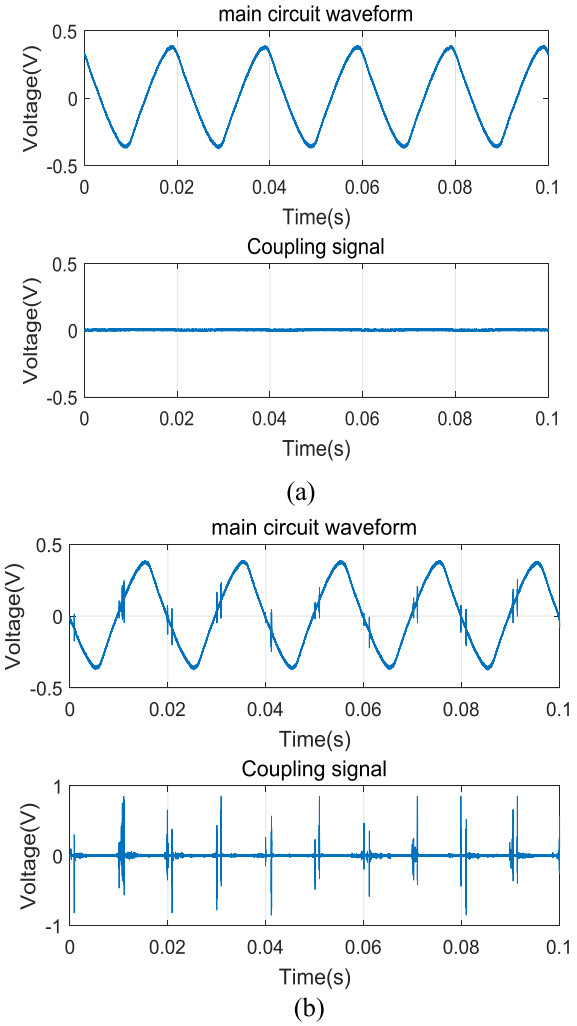

FIGURE 5. Analysis of missed judgment in the combined load. (a) each branch is normal. (b) arc faults in the rotary hammer branch.

IV. THE PRINCIPLE AND APPLICATION OF HIGHER ORDER STATISTICS

Higher-order statistics, that is, the statistics is higher than the first-order and second-order (such as the mean, variance, power spectrum and autocorrelation function), including the higher-order moments, the higher-order cumulants and the higher-order spectra. The stochastic process of the arc fault occurs with many non-Gaussian and non-linear signals. The second-order statistics are inherently defective due to the lack of phase information. The higher order statistics is not sensitive to Gaussian noise and can theoretically suppress Gaussian noise, which can be used to obtain more useful information. Presently, higher-order cumulants have been widely used in the fields of voice processing and fault diagnosis [24]–[27]. The fourth-order cumulant kurtosis information is used in this paper to analyze the arc-coupled signal data. The derivation process is as follows [28]:

x is assumed as a stationary random signal and

$$x_1 = x(t), \quad x_2 = x(t+\tau_1), \cdots x_k = x(t+\tau_{k-1}) \tag{2}$$

where τ is the amount of delay.

The k-th moment of the random signal is defined as follows:

$$m_k(\tau_1 \cdots \tau_{k-1}) = E[x(t)x(t+\tau_1)\cdots x(t+\tau_{k-1})] \tag{3}$$

The higher order moments can be used to characterize the higher order cumulants of the random signal. For the zero-mean signal, the fourth order cumulants of the random signal is

$$\begin{aligned} c_4(\tau_1,\tau_2,\tau_3) = {} & m_4(\tau_1,\tau_2,\tau_3) - m_2(\tau_1)\cdot m_2(\tau_3-\tau_2) \\ & - m_2(\tau_2)\cdot m_2(\tau_3-\tau_1) \\ & - m_2(\tau_3)\cdot m_2(\tau_2-\tau_1) \end{aligned} \tag{4}$$

When $\tau_1 = \tau_2 = \tau_3 = 0$, the above formula provides:

$$\begin{aligned} c_4(0,0,0) &= m_4(0,0,0) - 3m_2^2(0) \\ &= E[x^4(t)] - 3\{E[x^2(t)]\}^2 \end{aligned} \tag{5}$$

$c_4(0,0,0)$ is called as the kurtosis of the random signal; the normalized kurtosis K of the zero-mean random signal is defined as follows:

$$K = \frac{E[(x)^4] - 3\{E[(x)^2]\}^2}{\{E[(x)^2]\}^2} = \frac{1}{N}\sum_{i=1}^{N}\left(\frac{x_i - \bar{X}}{\sigma_x}\right)^4 - 3 \tag{6}$$

where $\bar{X} = \frac{1}{N}\sum_{i=1}^{N} x_i$, σ_x is the standard deviation and N is the length of the signal.

From the above definition we can see that the normalized kurtosis K is the ratio of the fourth-order cumulants of the signal to the square of the variance. The kurtosis value can describe the probability density distribution of the signal, which is a simple and effective statistic of the non-Gaussian random variable [28]. Therefore, this paper uses the kurtosis K to characterize the non-Gaussian process of the arc fault.

For a Gaussian signal, let x be a Gaussian random variable with a zero mean and a variance of σ^2. Then, the probability density function is

$$f(x) = \frac{1}{\sqrt{2\pi}\sigma}\exp(-\frac{x^2}{2\sigma^2}) \tag{7}$$

The moment generating function of x is

$$\phi(\omega) = \int_{-\infty}^{\infty} f(x)e^{j\omega x}dx = \frac{1}{\sqrt{2\pi}\sigma}\int_{-\infty}^{\infty}\exp(-\frac{x^2}{2\sigma^2} + j\omega x)dx \tag{8}$$

Using the integral formula:

$$\int_{-\infty}^{\infty}\exp(-Ax^2 \pm 2Bx - C) = \sqrt{\frac{\pi}{A}}\exp(-\frac{AC - B^2}{A}) \tag{9}$$

(8) can be transformed as follows:

$$\phi(\omega) = \exp(-\frac{\sigma^2\omega^2}{2}) \tag{10}$$

The logarithm of the moment generating function is the cumulative moment generating function for a Gaussian random variable, which is obtained from the above equation:

$$\psi(\omega) = \ln\phi(\omega) = \ln\exp(-\frac{\sigma^2\omega^2}{2}) = -\frac{\sigma^2\omega^2}{2} \tag{11}$$

The derivative of each order is

$$\begin{aligned} \psi^{(1)}(\omega) &= -\sigma^2\omega \\ \psi^{(2)}(\omega) &= -\sigma^2 \\ \psi^{(k)}(\omega) &\equiv 0, \quad k = 3,4,\cdots \end{aligned} \tag{12}$$

Let $\omega = 0$, each order cumulants of Gaussian random variables is

$$c_1 = 0, \quad c_2 = \sigma^2, \quad c_k = 0, \quad k = 3,4,\cdots \tag{13}$$

From the above analysis, the higher order cumulants of any Gaussian processes is zero, so the kurtosis of the Gaussian process is zero. In an actual operation, the kurtosis value cannot be completely ideal due to signal clutter or other external interference. For the random variable of the approximate Gaussian process, the kurtosis value should be near zero. When an arc fault occurs, the shock signal appears in the coupling signal, causing change of the probability density function. The amplitude distribution deviates from the normal distribution and the normal curve becomes sharp. The fourth-order cumulant kurtosis value is the reflection of the steepness of the normal curve. When the normal curve becomes abrupt and sharp, the kurtosis value is greatly increased.

V. IDENTIFICATION OF SERIES ARC FAULTS

The characteristic frequency of the coupling signal is analyzed by means of FFT method. With the present experimental conditions, The observation window of the oscilloscope is set as 20ms and the sampling rate of the oscilloscope is 50MHz to get a spectral resolution of 1/0.02=50Hz. Fig. 6, which is obtained through the analysis of the secondary circuit, shows that the characteristic frequency can reach MHz(around 2.5MHz).

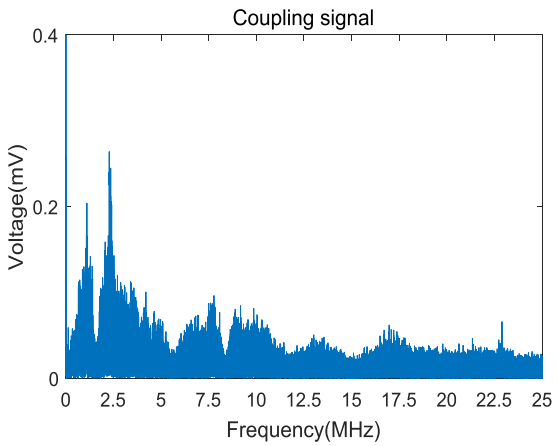

FIGURE 6. Spectrum of coupling signal of arc faults.

And then, the observation window of the oscilloscope is set as 100ms and the sampling rate of the oscilloscope is 10MHz. An analog low-pass filter is used to suppress noise signals and its cut-off frequency is 4MHz. By the analysis of the fourth-order cumulants of the data from the oscilloscope, each kurtosis is calculated in matlab.

A. SINGLE LOAD

The typical loads, which consist of an incandescent lamp (resistive), a rotary hammer (inductive) and a microwave oven (non-linear), are taken as examples, and the waveform of the coupling signal is analyzed as shown in Fig. 7. It can be seen that there are some commonalities before and after the arc under different types of loads: the normal coupling signal is an approximately stationary signal with zero mean.

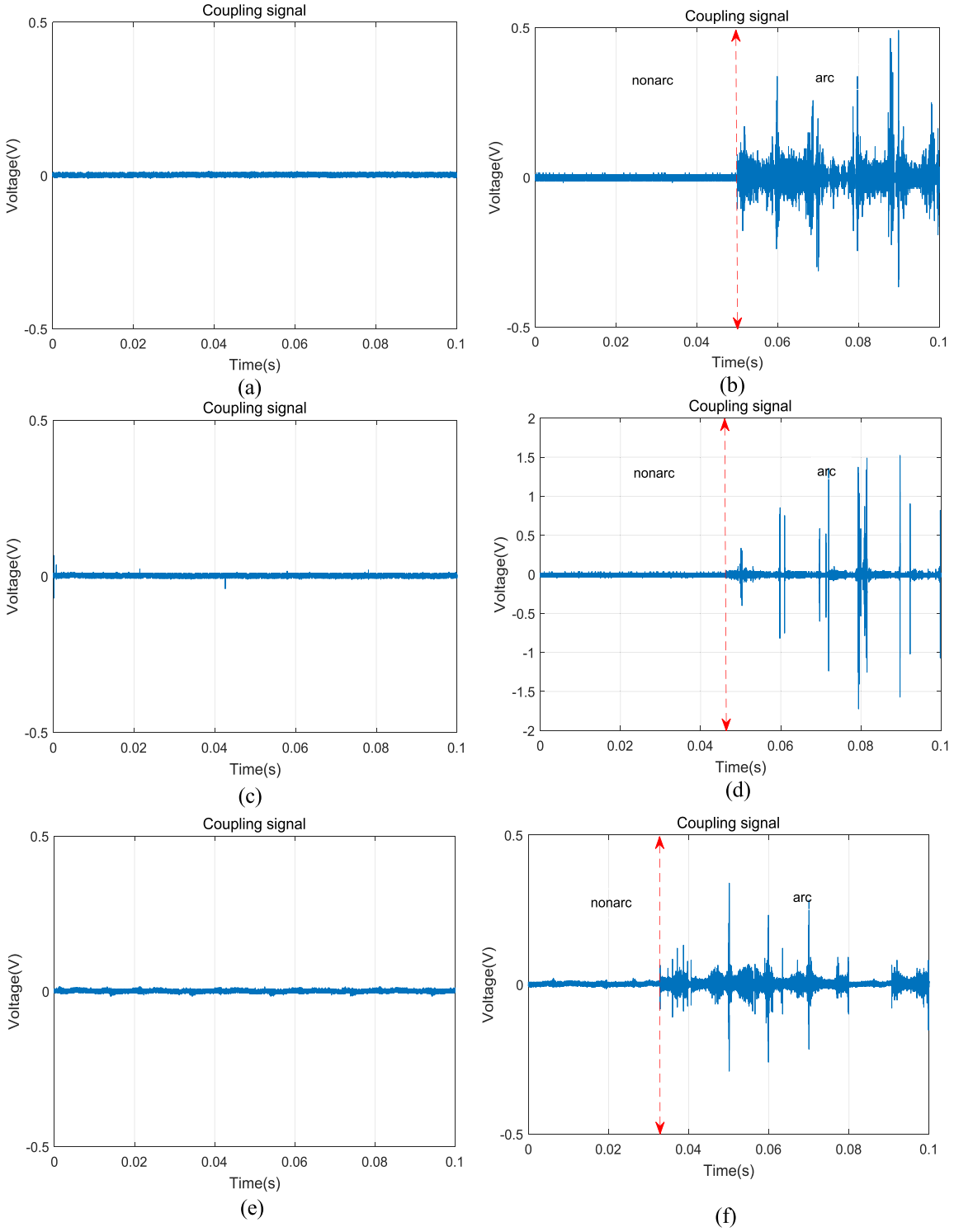

FIGURE 7. Analysis of the normal and arc fault coupling signals for a single load. (a) Incandescent lamp – normal. (b) Incandescent lamp - arc fault. (c) rotary hammer – normal. (d) rotary hammer - arc fault. (e) microwave oven- normal. (f) microwave oven- arc fault.

The amplitude of the coupling signal cannot exactly equal 0 due to the influence of line clutter.

The difference of the arc waveforms for different loads is as follows: In the case of inductive and non-linear loads, the pulse amplitude is larger, and the distribution is denser than the resistive load. This is due to the short zero crossing time in inductive loads, making the arc more intense and more difficult to extinguish, and the induced electromotive force

would prevent the circuit from breaking and form multiple arcs for the high frequency electromagnetic energy, which are expressed as a high-frequency burst. Additionally, the recovery voltage of the arc gap in inductive loads contains the transient component to show oscillation process. The high-frequency characteristics of the arc current are more obvious, and non-linear loads contain different degrees of inductive components.

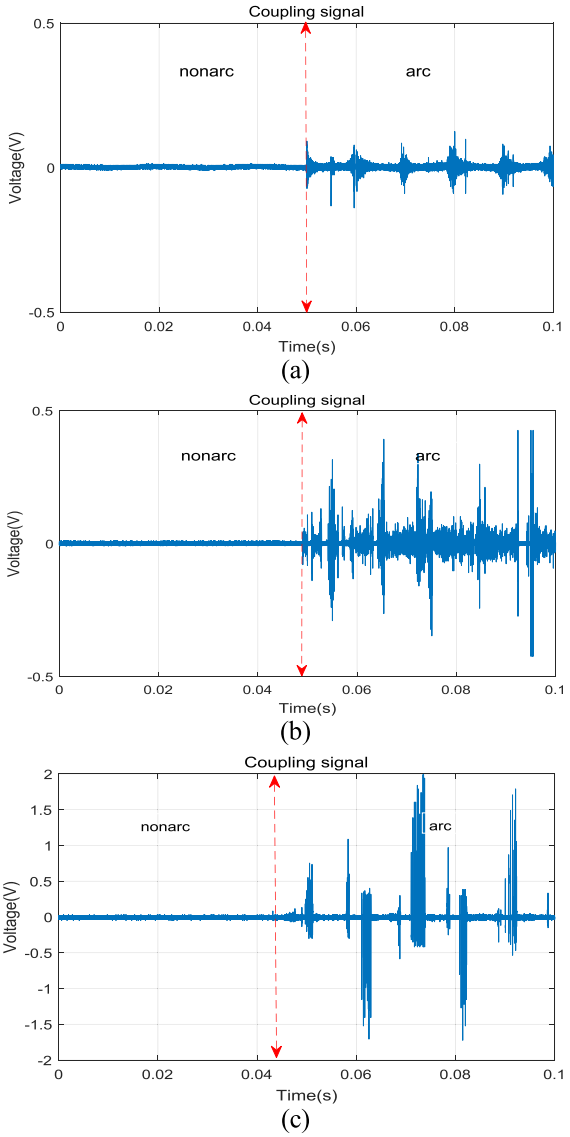

FIGURE 8. Coupling signal analysis of the trunk fault for the combined load. (a) a kettle + a refrigerator. (b) an incandescent lamp + a monitor. (c) a rotary hammer + a monitor.

B. TRUNK LOAD

The typical combinations are taken as examples including a kettle + a refrigerator (resistive + inductive), an incandescent + a computer screen (resistive + non-linear) and a rotary hammer + a computer screen (inductive + non-linear). The coupling signal waveforms are analyzed and the results are shown in Fig. 8. The kettle's power (1800 W) is larger than that of the refrigerator (250 W). Then, the combination is resistive dominantly so that the pulse wave exhibits similar fault characteristics as that of single resistive loads. However, to some extent, the involvement of the resistance increases pulse intensity of the combination. The power of the loads (an incandescent lamp + a monitor) and the characteristics are identical. The combination of a rotary hammer + a monitor is inductive and non-linear (mutual superposition) so that the fault pulse signal is very strong. From many experiments, the combined loads share similar arc fault features with the single loads.

TABLE 1. Fourth - order cumulant kurtosis of the coupling signal.

Load information	Test time(s)	Normal	Arc fault
resistive(kettle)	100	<1	>10
inductive(refrigerator)	100	<1	>195
non-linear(vacuum cleaner)	100	<1	>29
resistive + inductive (kettle + refrigerator)	100	<1	>10
resistive + non-linear (incandescent lamp + monitor)	100	<1	>29
inductive + non-linear (rotary hammer + monitor)	100	<1	>10
resistive + inductive (kettle + rotary hammer)	100	<1	~
kettle(1)+rotary hammer(0)	100	~	>10
kettle(0)+ rotary hammer (1)	100	~	>187
resistive + non-linear (kettle + fluorescent light)	100	<1	~
kettle(1) + fluorescent light(0)	100	~	>10
kettle(0) + fluorescent light(1)	100	~	>240
Inductive + non-linear (refrigerator + fluorescent light)	100	<1.3	~
refrigerator(1)+fluorescent light(0)	100	~	>95
refrigerator(0)+fluorescent light(1)	100	~	>85

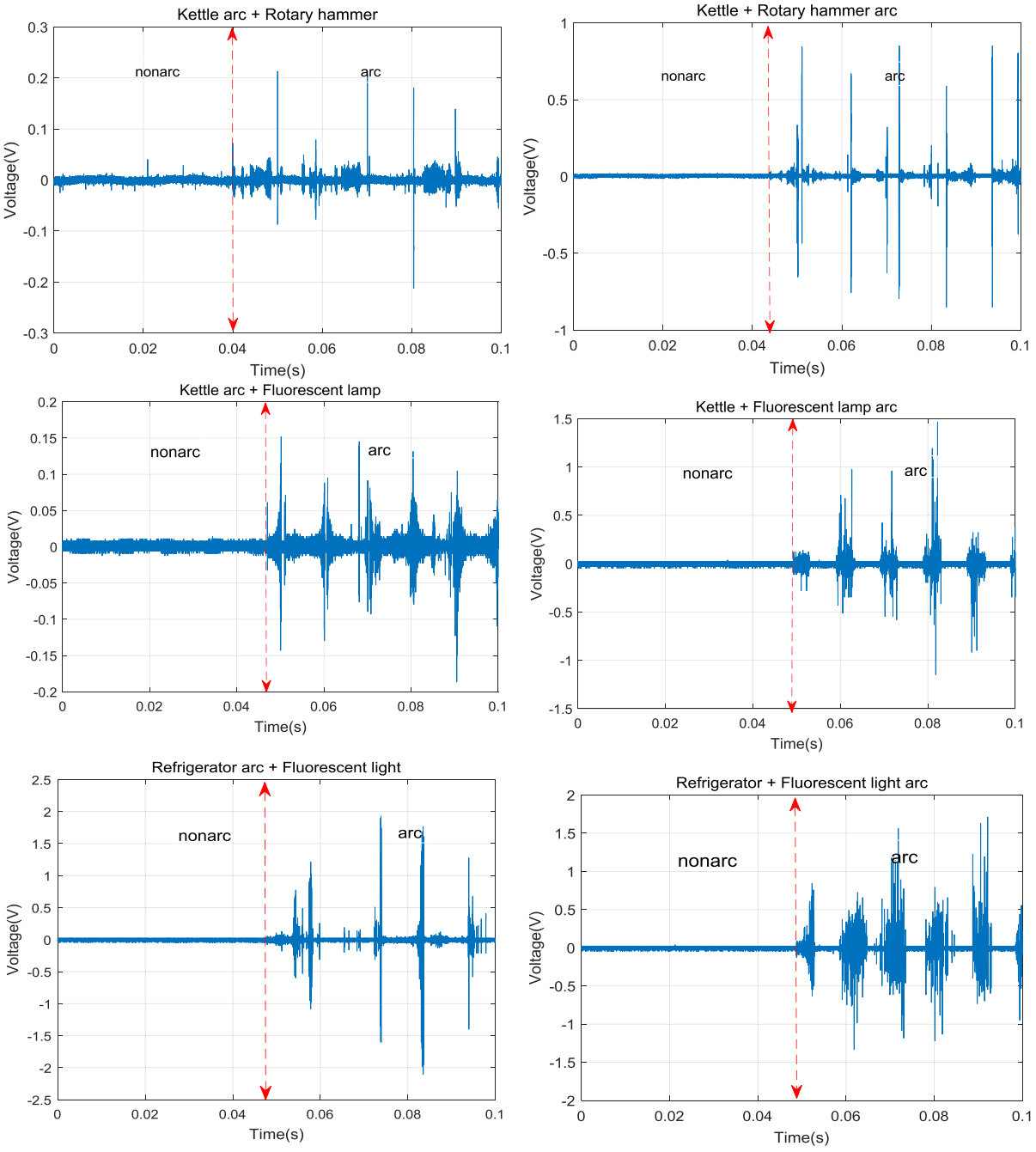

FIGURE 9. Coupling signal analysis of the branch fault for the combined load.

C. BRANCH FAULT IN COMBINED LOAD

The arc faults of the branch for each integrated load are experimentally investigated. The coupling signal waveforms of the main circuit before and after the arc are shown in Fig. 9. The arc characteristics of the branch can be seen to be similar to those of the corresponding single load. Due to the certain randomness of the arcing process, the arc did not continue burning so that there is a pulse interruption at around 0.075 s and 0.095 s in the kettle + rotary hammer load. For the 11 W fluorescent lamp, when its branch arc faults occur, the fault signal is more obvious, which will not cause missed judgment.

D. ARC IDENTIFICATION

Like the above cases, the coupling signal data are counted with higher-order statistics, and the kurtosis values are calculated. Each load is tested 100 times(50 times under the normal, 50 times under the arcing). The kurtosis table is shown in Table 1, where 1 means an arc and 0 means nonarc in the branch fault experiments of the integrated loads.

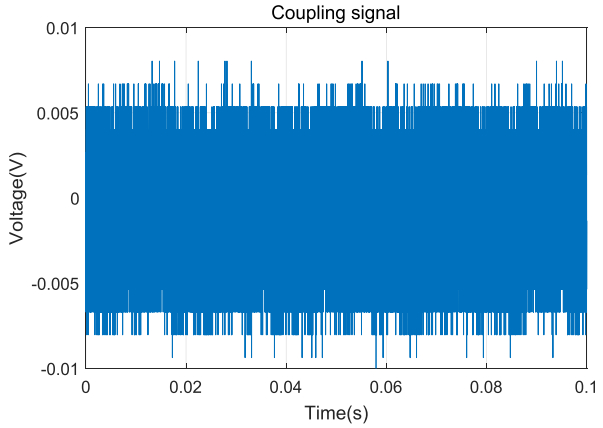

FIGURE 10. Amplification analysis of the normal coupling signal.

TABLE 2. Times of value greater than the set kurtosis threshold in 20 times of calculations.

load	starting	Arc fault
kettle	1	11
incandescent lamp	1	12
impact drill	1	20
refrigerator	3	20
vacuum cleaner	1	20
microwave oven	1	20
monitor	1	18
energy saving lamps	1	20
air compressor	1	20
incandescent + air compressor	1	18
vacuum cleaner+ air compressor	1	20

From Table 1, it can be seen that the maximum value of the normal state kurtosis is 1.3 and the minimum value of the fault state is 10. There is a significant difference between them.

In theory, the coupling signal in the normal state should be approximately 0, and the kurtosis value should be zero. However, there is a certain deviation of the table kurtosis values in some cases; the normal coupling signal waveform is analyzed at a smaller scale. An integrated load (a monitor + a rotary hammer) being taken as an example, the results are shown in Fig. 10. It can be seen that the line coupling signal is not completely 0 under its normal operation, and the kurtosis value of the signal has some deviation due to the influence of clutter. However, its amplitude is very small,

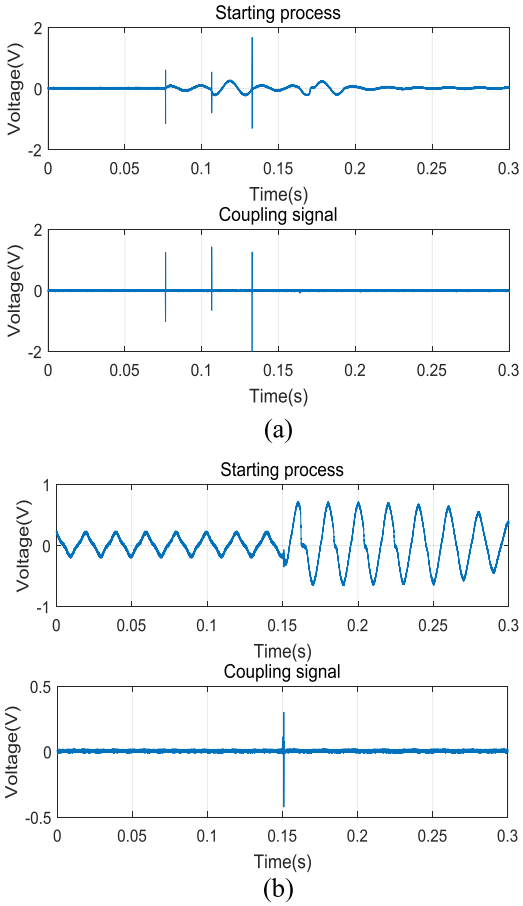

FIGURE 11. Analysis of the load starting process. (a) refrigerator. (b) vacuum cleaner + air compressor.

so the kurtosis deviation is not too large and oscillated about a value of 0. This is related to the effect of the actual experimental line clutter, but it does not affect arc identification. Through the above analysis and the analysis of section IV, it can be seen that the kurtosis value of the coupling signal in normal operation is approximately 0 and the kurtosis value is greatly increased when the arc faults occur. By combining the experimental results in the table, the kurtosis value can be set as 5 to distinguish between the normal and the arcing.

In all cases, the fault kurtosis values are greater than 10 but have some differences. This is because the kurtosis value is related to the number of pulses and the amplitude of the mutation. When the number of detected pulses is large, the kurtosis value is also large. When the sudden large pulse is detected, the kurtosis value increases rapidly.

E. STARTING PROCESS

Unfortunately, the starting of a certain load could often leads to unwanted judgment when there is no arc present. Through the examples of the refrigerator and vacuum cleaner + air compressor, the waveforms of their starting process are shown in Fig. 11. It can be seen from (a) that the pulse signal is detected in the coupling signal acquisition, which is similar

to the arcing signal and can cause misjudgment. However, irregular fluctuations in the starting current only occur in a very short period of time. By setting several times to detect the pulse signal, misjudgment can be effectively avoided. Fig(b) shows that the air compressor suddenly starts when the vacuum cleaner is under normal operation. The coupled signal pulse only appears at the instant of starting. According to the UL1699 standard (It is judged as arc fault if 8.5 cycles of current signal are abnormal within 0.5s), the kurtosis calculation is performed for every 25 ms of data collection. If there are 6 times of kurtosis anomalies within 0.5s (20 times of kurtosis calculations), the arc fault is identified. Each load is tested on starting process and the results are shown in table 2. For example, The number of the value greater than threshold in 20 times is only one during the starting process of the kettle load.

VI. CONCLUSION

In this paper, a method based on coupling signal acquisition and higher order cumulant recognition is proposed for the shortcomings of the main circuit current detection method. Through the analysis of arc faults in a single load, a trunk fault and a branch fault in a combined load and the starting process, the following conclusions are drawn:

1) The circuit current contains large high-frequency components when the arc is extinguished and reignited, and the electromagnetic field produced by a high-frequency current is coupled to the measurement circuit through the transformer coil and the signal shows the pulse waveform. Additionally, the frequency of the normal current signal is low so that the coupling signal is approximately 0. There is a clear distinction in the time domain between the normal and the arc fault statues, which will not cause faulty judgment.

2) When the high-frequency current is generated by the branch arc, the high-frequency current is also present in the trunk current and its electromagnetic field produces the coupling pulse signal. Therefore, this method can solve the failure-to-trip situations in the low power branch.

3) Through the analysis of the fourth-order cumulant kurtosis, the kurtosis is greatly increased when the arc fault occurs, which is obviously different from the kurtosis value of the normal statues. Therefore, setting a common kurtosis threshold and using continuous detection can effectively identify the arc faults.

4) This method avoids the rated current singularity of all kinds of loads, and the type of load does not need to be judged. The threshold does not change with the change of the load type, which can be used as a new approach for series arc fault detection.

REFERENCES

[1] *China Fire Yearbook (2015)*, China Personnel Publishing House, Beijing, China, 2015.

[2] U.S. Fire Administration. (Mar. 11, 2014). *FEMA2014, Residential Building Fires (2009-2011). Topical Fire Report Series*. [Online]. Available: http://www.usfa.fema.gov/downloads/pdf/statistics/v14i13.pdf

[3] C. E. Restrepo, "Arc fault detection and discrimination methods," in *Proc. 53rd IEEE Holm Conf. Elect. Contacts*, Pittsburgh, PA, USA, Sep. 2007, pp. 115–122.

[4] S. Panetta, "Design of arc flash protection system using solid state switch, photo detection, with parallel impedance," in *Proc. IEEE IAS Elect. Saf. Workshop*, Dallas, TX, USA, Mar. 2013, pp. 211–213.

[5] M. Zhen, W. Li, and Q. Sun, "The characteristics of DC arc faults current," in *Proc. 15th Eur. Conf. Power Electron. Appl. (EPE)*, Lille, France, Sep. 2013, pp. 1–9.

[6] D. C. Mohla, T. Driscoll, P. S. Hamer, and S. A. R. Panetta, "Mitigating electric shock and arc-flash energy: A total system approach for personnel and equipment protection," *IEEE Ind. Appl. Mag.*, vol. 18, no. 3, pp. 48–56, May/Jun. 2012.

[7] G. Artale, A. Cataliotti, V. Cosentino, D. Di Cara, S. Nuccio, and G. Tiné, "Arc fault detection method based on CZT low-frequency harmonic current analysis," *IEEE Trans. Instrum. Meas.*, vol. 66, no. 5, pp. 888–896, May 2017.

[8] A. Mukherjee, A. Routray, and A. K. Samanta, "Method for online detection of arcing in low-voltage distribution systems," *IEEE Trans. Power Del.*, vol. 32, no. 3, pp. 1244–1252, Jun. 2017.

[9] Q. Xiong, S. Ji, L. Zhu, L. Zhong, and Y. Liu, "A novel DC arc fault detection method based on electromagnetic radiation signal," *IEEE Trans. Plasma Sci.*, vol. 45, no. 3, pp. 472–478, Mar. 2017.

[10] J. J. Dougherty, "Circuit breaker with arc fault detection and method of operation," U.S. Patent 8 213 138, Jul. 3, 2012.

[11] N. Hadziefendic, M. Kostic, Z. Radakovic, "Detection of series arcing in low-voltage electrical installations," *Eur. Trans. Electr. Power*, vol. 19, pp. 423–432, Apr. 2009.

[12] J. L. Calvo, P. Schweitzer, S. Weber, E. Tisserand, and P. Joyeux, "Arcing detection at home system using correlation analysis," in *Proc. 27th Int. Conf. Elect. Contacts (ICEC)*, Dresden, Germany, Jun. 2014, pp. 1–6.

[13] J. Lezama, P. Schweitzer, E. Tisserand, J.-B. Humbert, S. Weber, P. Joyeux, "An embedded system for AC series arc detection by inter-period correlations of current," *Electr. Power Syst. Res.*, vol. 129, pp. 227–234, Dec. 2015.

[14] J. Lezama, P. Schweitzer, S. Weber, E. Tisserand, and P. Joycux, "Arc fault detection based on temporal analysis," in *Proc. IEEE 60th Holm Conf. Elect. Contacts (Holm)*, New Orleans, LA, USA, Oct. 2014, pp. 1–5.

[15] E. Tisserand, J. Lezama, P. Schweitzer, and Y. Berviller, "Series arcing detection by algebraic derivative of the current," *Electr. Power Syst. Res.*, vol. 119, pp. 91–99, Feb. 2015.

[16] Y. Liu, F. Guo, Z. Wang, C. Cehn, and Y. Li, "Research on the spectral characteristics of series arc fault based on information entropy," *Trans. China Electrotech. Soc.*, vol. 30, no. 12, pp. 488–495, 2015.

[17] J. Yong, X. Gui, and L. Niu, "Series arc fault identification in low voltage system based on autoregressive parameter model," *Trans. China Electrotech. Soc.*, vol. 26, no. 8, pp. 213–219, 2011.

[18] S. Jamali and N. Ghaffarzadeh, "A new method for arcing fault location using discrete wavelet transform and wavelet networks," *Eur. Trans. Electr. Power*, vol. 22, no. 5, pp. 601–615, 2012.

[19] I. Baqui, I. Zamora, J. Mazón, and G. Buigues, "High impedance fault detection methodology using wavelet transform and artificial neural networks," *Electr. Power Syst. Res.*, vol. 81, no. 7, pp. 1325–1333, 2011.

[20] S. H. Ma, J. Q. Bao, and Z. Y. Cai, "A novel arc fault identification method based on information dimension and current zero," *Proc. CSEE*, vol. 36, no. 9, pp. 2572–2579, 2016.

[21] Z. Xu, *Foundation Theory of Electrical Appliances*. Beijing, China: China Machine Press, 2014, pp. 139–140.

[22] C. J. Kim, "Electromagnetic radiation behavior of low-voltage arcing fault," *IEEE Trans. Power Del.*, vol. 24, no. 1, pp. 416–423, Jan. 2009.

[23] Y. Kayano, H. Miura, K. Miyanaga, and H. Inoue, "The relationship between voltage and duration of short-time arc generated by slowly breaking silver contact," *IEICE Trans. Electron.*, vol. E91-C, no. 8, pp. 1230–1232, 2008.

[24] O. N. Gerek and D. G. Ece, "Power-quality event analysis using higher order cumulants and quadratic classifiers," *IEEE Trans. Power Del.*, vol. 21, no. 2, pp. 883–889, Apr. 2006.

[25] J. J. G. de la Juan *et al.*, "Higher-order characterization of power quality transients and their classification using competitive layers," *Measurement*, vol. 42, no. 3, pp. 478–484, 2009.

[26] R. Shao, J. Li, W. Hu, and F. Dong, "Multi-fault clustering and diagnosis of gear system mined by spectrum entropy clustering based on higher order cumulants," *Rev. Sci. Instrum.*, vol. 84, no. 2, p. 025107, 2013.

[27] Y. Wang, J. Fan, and Y. Yao, "Online monitoring of multivariate processes using higher-order cumulants analysis," *Ind. Eng. Chem. Res.*, vol. 53, no. 11, pp. 4328–4338, 2014.
[28] X. Zhang, *Modern Signal Processing*. Beijing, Chiana: Tsinghua Univ. Press, 2002.

GUANGHAI BAO received the B.S. and Ph.D. degrees in electrical engineering from Fuzhou University, Fujian, China, in 2000 and 2011, respectively. He held a Postdoctoral position with Changshu Switching Manufacturing Co., Ltd. He is currently an Associate Professor and the Department Head with the College of Electronic Science and Engineering, Fuzhou University. His current research interest include electrical appliances and fault diagnosis.

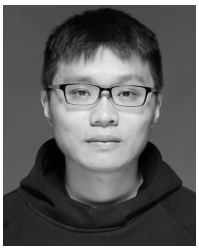

RUN JIANG received the B.S. degree from Fuzhou University, Fujian, China, in 2016, where he is currently pursuing the master's degree. His current research interests includes the detection of arc faults.

DEJUN LIU received the B.S. degree from Fujian Agriculture and Forestry University, Fujian, China, in 2015, and the M.S. degree from Fuzhou University, Fujian, in 2018. He is currently with Quanzhou Power Supply Bureau of State Grid, Fujian. His current research interests include smart appliances and online monitoring technology.